Substorm onset by new plasma intrusion: THEMIS spacecraft observations

X. Xing,[1] L. Lyons,[1] Y. Nishimura,[1,2] V. Angelopoulos,[3] D. Larson,[4] C. Carlson,[4] J. Bonnell,[4] and U. Auster[5]

Received 25 April 2010; revised 30 June 2010; accepted 6 July 2010; published 27 October 2010.

[1] Recent observations from the 2-D array of high-resolution THEMIS all-sky imagers (ASIs) during the 2008 tail season have shown that the majority of substorm onsets are preceded by equatorward extension of an auroral arc initiated at the poleward boundary of the aurora zone, and that the aurora breakup is likely triggered when this precursor arc reaches the onset region. These observations were used to suggest that substorm onset is driven by a new population of plasma having lower global entropy content than that of the preexisting plasma intruding into the inner plasma sheet. We have taken advantage of conjunctions between the location of the precursor arc observed by the THEMIS ASI and THEMIS spacecraft and identified four events where clear signatures of the proposed new plasma intrusion were observed simultaneously in both the magnetotail and ionosphere. In two of the events, the intrusion plasma was captured more than 10 min before substorm onset in the midtail plasma sheet. The intruding plasma is characterized as the reduction of the pressure and entropy parameter associated with more dipolarized magnetic field, as well as the enhancement of the duskward electric field and earthward flow. In two other events, the plasma intrusion was found within 2 min before onset in the inner plasma sheet region R ~11 R_E, which is very close to the onset locations. These observations are consistent with the proposal that intrusion of low-entropy content plasma to the onset region may provide a trigger for substorm onset. We also found two plasma intrusion events not associated with substorm onset in the plasma sheet, which indicates that the new plasma intrusion is not a sufficient condition for substorm onset. We suggest that sufficient pressure and azimuthal pressure gradient buildup in the inner plasma sheet during growth phase should be another necessary condition.

Citation: Xing, X., L. Lyons, Y. Nishimura, V. Angelopoulos, D. Larson, C. Carlson, J. Bonnell, and U. Auster (2010), Substorm onset by new plasma intrusion: THEMIS spacecraft observations, *J. Geophys. Res.*, *115*, A10246, doi:10.1029/2010JA015528.

1. Introduction

[2] The substorm timing sequence has been a controversial topic for several decades, with different onset processes being supported using different spacecraft and ground-based data sets [e.g., *McPherron et al.*, 1973; *Lyons*, 1995; *Angelopoulos et al.*, 2008; *Lui*, 2008]. The spatial coverage of a spacecraft is always very limited, even with multi-spacecraft missions [e.g., *Escoubet et al.*, 1997; *Angelopoulos*, 2008]. Ionospheric observations by images and radars are powerful tools that supplement spacecraft observations, providing 2-D imaging of aspects of plasma sheet dynamics [e.g., *Henderson et al.*, 1998; *Sergeev et al.*, 1999; *Zesta et al.*, 2002], except that the density of ground-based auroral imagers was limited. However, the situation has recently changed with the deployment of the extensive network of THEMIS high-resolution all-sky imagers (ASIs).

[3] *Nishimura et al.* [2010] has taken advantage of the THEMIS all-sky imager array to study the low-intensity preonset aurora activity, which might be missed in earlier studies. They surveyed the 2008 THEMIS tail season data and found that more than 80% of the aurora onsets were preceded by equatorward-moving approximately north-south (N-S)-oriented auroral arcs extending from poleward boundary intensifications (PBIs) initiating 5.5 min on average prior to the onset. They suggested that the east-west component of the orientation of these preonset arcs was determined by the

[1]Department of Atmospheric and Oceanic Science, University of California, Los Angeles, Los Angeles, California, USA.
[2]Solar-Terrestrial Environment Laboratory, Nagoya University, Furocho, Chikusa, Nagaya, Japan.
[3]Institute of Geophysics and Planetary Physics/Earth and Space Sciences, University of California, Los Angeles, Los Angeles, California, USA.
[4]Space Sciences Laboratory, University of California, Berkeley, Berkeley, California, USA.
[5]Institut für Geophysik und Extraterrestrische Physik der TUBM 3, Braunschweig, Germany.

0148-0227/10/2010JA015528

convection cell that the arc follows. Furthermore, by using ground radar, *Lyons et al.* [2010] provided evidence that equatorward flow enhancements associated with reduced E-region densities, which may represent the reduced entropy plasma, enter the aurora oval from the polar cap ~8 min prior to the onset and reach the onset location just before the onset. These studies suggested that the preonset auroral structures reflect flowing plasma that plays an important role in leading to the substorm onset.

[4] The large-scale equatorward extension of the N-S auroral arcs has been suggested to be associated with earthward fast flow channels [*Lyons et al.*, 1999; *Fairfield et al.*, 1999; *Nakamura et al.*, 2001; *Kauristie et al.*, 2003] or bursty flows [*Baumjohann et al.*, 1990; *Angelopoulos et al.*, 1994]. The physics of the preonset aurora arcs observed by *Nishimura et al.* [2010] is expected to be identical with that of north-south-oriented auroral streamers, except that the preonset arcs can be of smaller scale and lower intensity. The fast flow channels can be interpreted by the plasma bubble theory proposed by *Pontius and Wolf* [1990] and *Chen and Wolf* [1993], where the field line entropy parameter $PV^{5/3}$ (P is the central plasma sheet thermal pressure and V is the flux tube volume defined by $V = \int \frac{ds}{B}$) is an important factor in understanding the plasma transport.

[5] Empirical models have suggested that the entropy parameter in the Earth's plasma sheet statistically increases tailward [*Garner et al.*, 2003; *Xing and Wolf*, 2007]. However, if the entropy parameter experiences a sudden decrease in the distant tail region, the reduced entropy flux tubes become interchange unstable against their surroundings and will thus penetrate toward the near-Earth plasma sheet to release potential energy [*Schmidt*, 1979; *Volkov and Mal'tsev*, 1986; *Xing and Wolf*, 2007]. The plasma within the flow channel experiences enhanced gradient-curvature drift as it approaches the near-Earth region and stops as it achieves pressure balance with its surrounding flux tubes [*Wolf et al.*, 2009]. As described by *Chen and Wolf* [1993], a reduced entropy flow channel should generally be associated with a more dipolarized magnetic field configuration than the surrounding plasma. An enhanced duskward electric field is expected to be within the flow channels, associated with region 1 sense field-aligned currents at the edges of the channel. Enhanced electron precipitation associated with the upward field-aligned current at the duskward edge of the flow channel is expected to be associated with the north-south auroral arcs observed in the ionosphere. If the correlation between the preonset aurora arcs found by *Nishimura et al.* [2010] and the plasma sheet flow channel can be confirmed, the flow channel may be a crucial factor in triggering the substorm onset.

[6] In this study, we investigate the THEMIS spacecraft data for the events found by *Nishimura et al.* [2010] to see if a preonset flow channel is present within the midtail and near-Earth plasma sheet as a magnetotail counterpart of the preonset N-S arcs. A clear correlation was found for several events with good conjunctions between the spacecraft and the expected equatorial mapping of the region adjacent to the preonset N-S aurora, and for which the spacecraft did not move repetitively in and out of the plasma sheet. Spacecraft data in early 2009 were also surveyed. No good conjunctions were found for preonset aurora arcs, however, reduced entropy fast flow was found for a few N-S arcs having good conjunctions during nonsubstorm periods. Finally, possible reasons why some fast flow channels associated with reduced entropy flux tubes lead to onset and some do not are discussed.

2. Data Set

[7] We have collected observations from four good conjunction events found by *Nishimura et al.* [2010] during 2008 THEMIS tail season [*Angelopoulos*, 2008] when preonset N-S auroral arcs were observed, and two conjunction events for nonsubstorm N-S arcs in early 2009. All four preonset events and one of the nonsubstorm events are discussed in detail in sections 3.1 and 3.2. During these events, at least one of the THEMIS spacecraft footprints was mapped to the vicinity of the N-S auroral arc in the ionospheric E-region using the magnetic field model with the input solar wind conditions obtained from OMNIWeb by *Tsyganenko and Stern* [1996, hereafter T96]. The statistical model mapping technique does not provide accurate footprint locations using instantaneous solar wind conditions, especially during large solar wind temporal variations. Thus, a certain range of footprint deviations should be allowed in addition to the model uncertainty itself. We estimated the footprint location range using different solar wind conditions referred from OMNIWeb to evaluate the possible mapping errors for the investigation of the conjunction events. All the events show evidence of earthward transport of reduced entropy plasma by fast flow channels associated with the N-S auroral arc observed by the THEMIS ASIs.

[8] Both the electrostatic analyzer [*McFadden et al.*, 2008] and solid state telescope particle detectors, which cover the particle energy range from 5 eV to 6 MeV for ions and 5 eV to 1 MeV for electrons, were used for particle pressure and flow measurements. The magnetic field and electric field data are taken from the flux gate magnetometer [*Auster et al.*, 2008] and the electric field instrument [*Bonnell et al.*, 2008].

3. Data Analysis

3.1. Preonset N-S Auroral Arcs

[9] The first event includes a preonset N-S auroral arc in conjunction with the THEMIS spacecraft located away from the center of the plasma sheet, where the fast flow channel signatures were captured associated with the N-S arc. Figure 1 shows six selected images from THEMIS ASI array in the Alaska sector on 4 February 2008, which is the second event (Figure 2) shown by *Nishimura et al.* [2010]. E-region mappings of the THEMIS B, C, D, and E spacecraft using instantaneous solar wind conditions are shown on each image. The green rectangle in the top middle image identifies the variation of the THC footprint calculated using different interplanetary magnetic field (IMF) input, for which the extremum of the IMF variations within ~30 min around the N-S arc time period were used. A substorm onset is identified by an auroral brightening at 1048:06 UT followed by a poleward expansion. The key features of the preonset sequence are summarized as follows: Prior to the onset at ~1036 UT, a PBI initiated in the INUV field of view (FOV) near ~75° magnetic latitude (MLAT). An auroral arc then extended equatorward and eastward from this PBI, which passed the vicinity of the possible THC footprint range between about

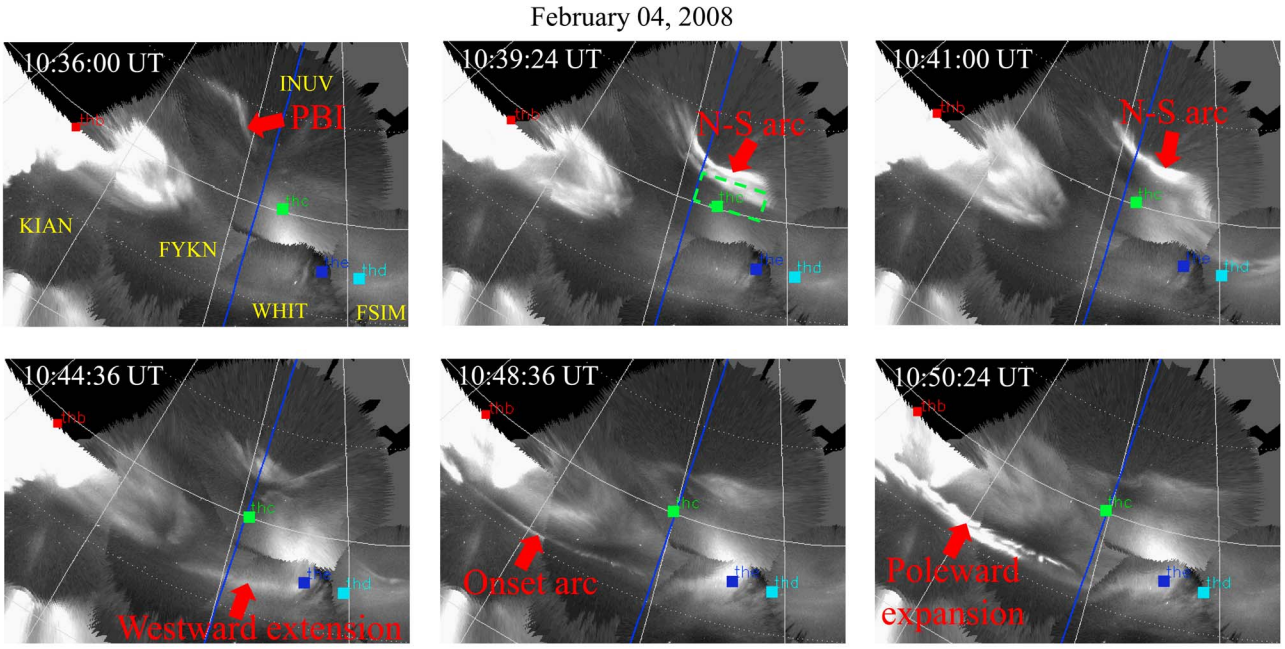

Figure 1. Snapshots of THEMIS ASI observations in the Alaskan sector on 4 February 2008. The spacecraft footprints are represented by squares (green for THC, cyan for THD, and blue for THE). The blue line represents the midnight meridian. The white lines represent isocontours of the magnetic latitude and longitude. The substorm onset occurred at 1048:06 UT.

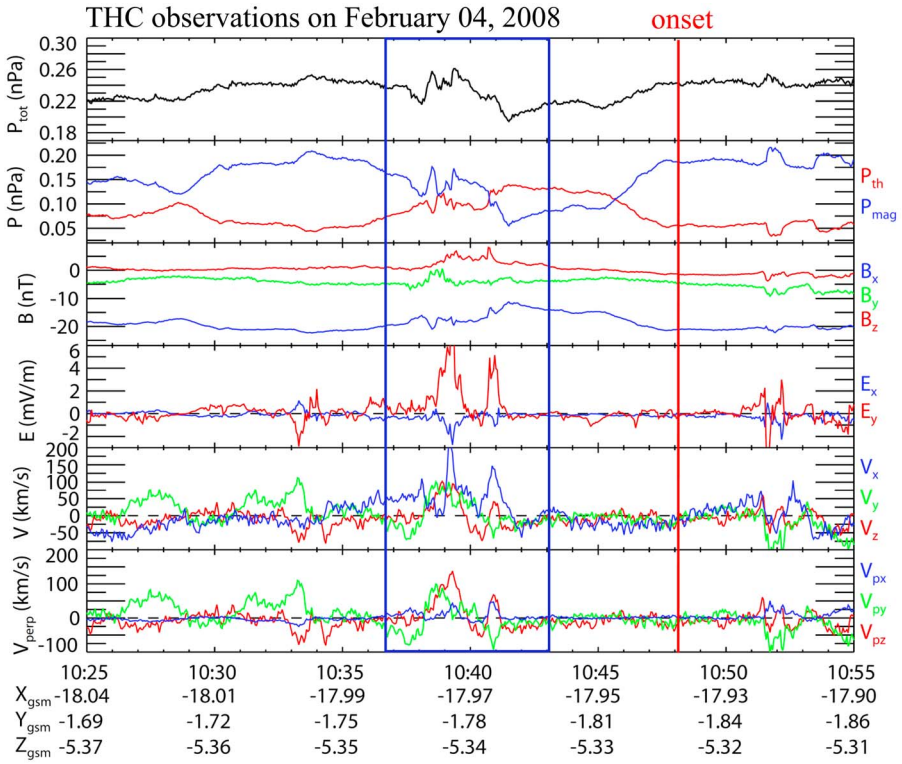

Figure 2. The THC spacecraft observations near the plasma sheet boundary layer on 4 February 2008 between 1025 and 1055 UT, corresponding to the aurora observations shown in Figure 1. The panels show total pressure, plasma and magnetic pressures, magnetic field, electric field, plasma bulk flow velocity, and perpendicular velocity in the GSM coordinates.

1039 and 1044 UT. After this N-S auroral arc contacted the preexisting growth phase arc near the equatorward boundary of the auroral oval at ~1043 UT, an auroral enhancement extended westward along the preexisting arc. The onset brightening started when the westward extending aurora propagated to the onset longitude, which was ~1 magnetic local time (MLT) to the west of the initial N-S auroral structure and ~2 MLT to the west of the location where this structure contacted the growth phase arc. The clockwise motion of the preonset arc in this event is suggested to be related to the plasma flow in the dusk convection cell around the Harang reversal region [*Nishimura et al.*, 2010], where substorm onset tends to occur [*Zou et al.*, 2009].

[10] Figure 2 shows the THC observations (GSM coordinates used throughout) at X ~−18 R_E near the midnight meridian between 1025:00 and 1055:00 UT. The blue rectangle marks the time interval between the PBI initiation and when the N-S auroral arc moved across the vicinity of the THC footprint region. The substorm onset time determined using the ASIs is identified by the vertical red line. The first panel displays the total pressure and the second panel shows the plasma thermal and magnetic pressures. The magnetic pressure was substantial near the beginning of the interval, indicating that the spacecraft was near the plasma sheet boundary; the thermal pressure became larger near the end of the interval. The third to the sixth panels show magnetic field, electric field, ion bulk flow velocity, and perpendicular flow velocity, respectively.

[11] The total pressure shows a small reduction following the PBI initiation between ~1036:00 and ~1038:00 UT and a substantial decrease between ~1039:24 and ~1041:30 UT when the N-S arc was within the vicinity of the THC footprint. Under an assumption of 1-D pressure balance in the Z_{GSM} direction, the central plasma sheet thermal pressure and the crosstail current are expected to be reduced associated with the total pressure reduction at this radial distance. The third panel shows the three components of the magnetic field. A several nanotesla enhancement of B_z, and thus enhancement of the magnetic field inclination, started ~1.5 min earlier than the major total pressure reduction. This represents a reduction of the magnetic field line stretching, which suggests a reduction of the flux tube volume. The entropy parameter cannot be calculated using the formula from the work of *Wolf et al.* [2006] because the spacecraft was too far away from the central plasma sheet in this case. However, it can be inferred from the pressure and magnetic field observations that the field line entropy parameter reduced when the flow channel-related aurora structure moved close to the location of the spacecraft mapping. The duskward electric field exhibits a substantial enhancement, which is exactly consistent with the magnetic field change and the ion bulk flow enhancement. The largest perpendicular component of the flow enhancement is essentially toward the central plasma sheet, which suggests plasma transport through the plasma sheet boundary toward the central plasma sheet and an earthward flow enhancement tailward of the spacecraft where the mapping of the spacecraft field line reached the central plasma sheet. The magnetic field and electric field temporal variations are slightly earlier than the major pressure reduction, perhaps reflecting variations along the magnetic field line ahead of the plasma transported to the spacecraft location.

[12] It is not certain what the earthward flow speed was within the equatorial plane, but it certainly should have been substantially greater than that seen at the spacecraft location due to the much smaller equatorial field. Adopting a ~200 km/s earthward-propagating velocity, the flow channel would have taken ~5 min to carry plasma from the spacecraft location to the inner plasma sheet boundary near X ~−8 R_E. Taking into account less than ~1 min Alfven transit time, the earthward propagation is roughly consistent with the time that the preonset N-S arc reached the auroral oval equatorward boundary at ~1043 UT.

[13] The spacecraft THD and THE, located more earthward and less than 1 MLT to the east of THC, did not observe any substantial changes, although their footprints were mapped to the vicinity of the eastward edge of the N-S aurora arc and near the equatorial growth phase arc by the T96 model. This could be due to the two spacecraft moving away from the central plasma sheet at this time due to the magnetic field stretching.

[14] The second event includes a preonset auroral arc in conjunction with the THEMIS spacecraft located near the center of the plasma sheet. Figure 3 shows six selected snapshots of THEMIS ASIs from six stations near the Churchill Line during a magnetic storm on 9 March 2008 between 0524:00 and 0542:00 UT. The footprints of THEMIS spacecraft THB, THC, THD, and THE are shown using fixed solar wind conditions obtained from OMNIWeb since large variations of instantaneous solar wind conditions during this time period bring unrealistic footprint variations. The THB footprint locations calculated using the extremum values of the IMF around this time period are identified by the red rectangle in the first image. Notice that the T96 magnetic field model is not an appropriate model for the storm time magnetotail, so that larger mapping uncertainty should be allowed. Thus, timing consistency between the spacecraft observations and the N-S aurora arc should be the key factor in estimating the spacecraft location. In this case, we focus more on the aurora arc slightly poleward of the THB footprint in the first image.

[15] This arc, having narrow longitudinal width, entered the SNKQ FOV before ~0515 UT. It initiated poleward of ~70° latitude to the west of the images in Figure 3 and propagated eastward and equatorward. The equatorward portion of this arc was oriented in the north-south direction and extended toward low latitudes eastward of the THB footprint before 0521 UT, which we marked as the first intensification (not shown). The second intensification, highlighted in the first and second images, initiated before ~0523 UT and diminished at ~0531 UT along the same aurora form. This second intensification along the arc approached closer to the spacecraft THB footprints between ~0523 and ~0528 UT. The third intensification initiated along the same arc at ~0532 UT and faded out before ~0538 UT. None of these three intensifications led to an onset. The fourth intensification started at ~0538:42 UT along the same arc and penetrated to the preexisting growth phase arc at ~60° magnetic latitude in the KAPU FOV, leading to a substorm onset at ~0541:12 UT. The N-S structure moved eastward as the third intensification started and kept moving toward the onset expansion region until the fourth intensification connected to that region.

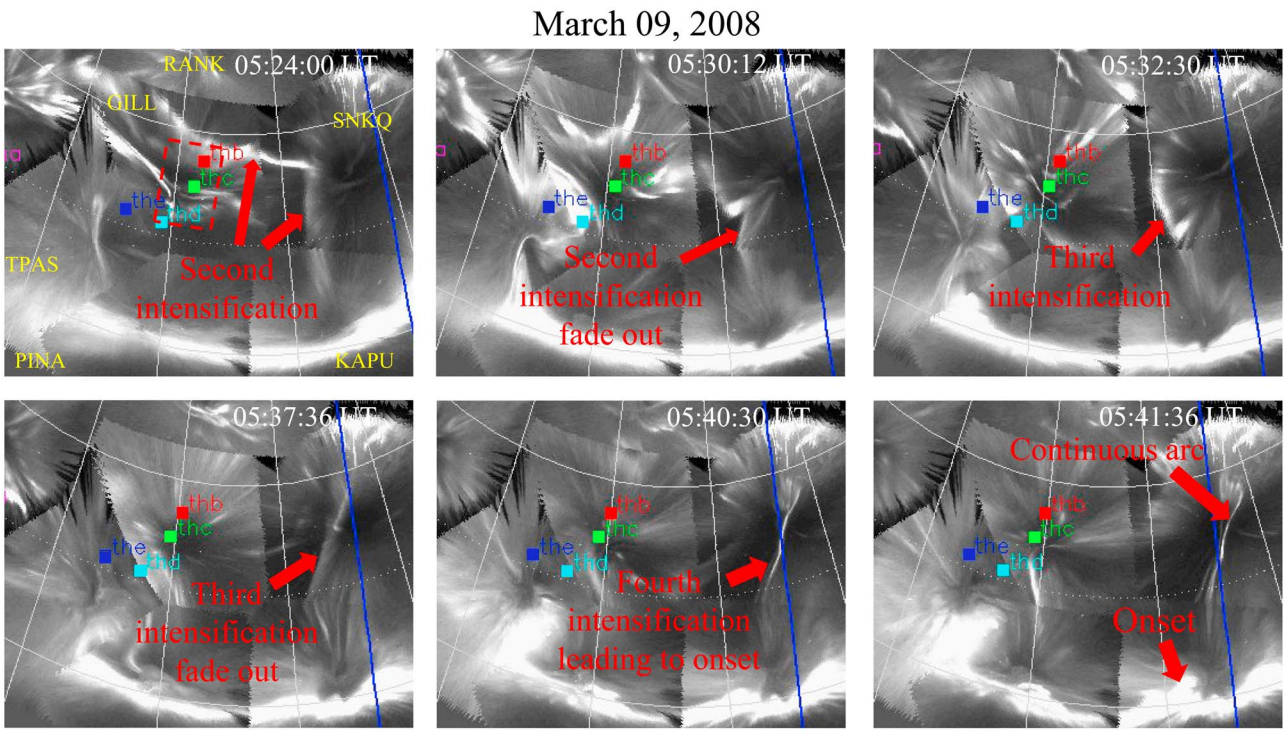

Figure 3. Snapshots of THEMIS ASI observations on 9 March 2008. The spacecraft footprints are represented by squares (red for THB, green for THC, cyan for THD, and blue for THE). The substorm onset occurred at 0541:36 UT.

[16] The aurora activity during this event is much more complicated than those during typical isolated substorms since this is a storm time event. There were several arcs that formed earlier than and to the west of the arc we focus on and were not connected to the onset signature at ~0541:12 UT discussed above for this event. These include a N-S arc that initiated at ~0513 UT within GILL FOV and penetrated into TPAS FOV at ~0525 UT. This arc led to a pseudo-breakup at ~0529 UT that was followed by a small onset expansion at ~0540 UT in the PINA and TPAS FOV. This onset was nearly 2 h west of the onset at ~0541:12 UT discussed above, and the auroral activity of that onset was not connected to that of the 0540:12 UT onset. The THB footprint was located poleward and eastward of this N-S arc. The timing consistency between the spacecraft observations (shown in Figure 4) and the N-S arc evolutions suggest that the flow channel observed by THB was part of the N-S arc sequence that connected to the KAPU onset.

[17] Figure 4 shows the observations from the THB spacecraft located at X ~−19 R_E in the premidnight sector. The seven panels show the total pressure, thermal and magnetic pressures, magnetic field, entropy parameter ($PV^{5/3}$, calculated using the model by *Wolf et al.* [2006]), electric field, ion density, and ion flow velocity, respectively. The substorm onset time determined using the ASIs is identified by the vertical red line. The blue rectangle marks the time interval between ~0523:00 and ~0528:00 UT, when the poleward portion of the N-S arc passed the vicinity of the THB footprint during the second intensification. Between ~0523:20 to ~0526:20 UT, the total pressure shows a moderate reduction with fluctuations. This reduction results from a thermal pressure decrease. The magnetic field shows a transient reconfiguration similar to a dipolarization signature but of shorter duration. The pressure reduction and local dipolarization are related to a substantial reduction of the entropy parameter in the fourth panel. The electric field shows simultaneous and substantial enhancements with the magnetic field and entropy changes. The ion density shows abrupt reduction during the same time period, and the ion flow shows substantial earthward and dawnward enhancements, which are consistent with the motion of the poleward portion of the aurora arc near 68° MLAT.

[18] Unfortunately, the flow channel captured by THB did not correspond to the fourth intensification along this aurora arc, which directly led to onset. However, it corresponded to an intensification along the same aurora arc and has all the expected plasma sheet properties of the preonset flow channel. The second auroral intensification did not reach as close to the equatorward aurora as did the fourth intensification, so that it is possible that this second flow enhancement observed by THB dissipated before reaching the plasma sheet inner boundary. Thus, it would be interesting to roughly estimate the radial distance where the second flow enhancement may have reached. Taking ~100 km/s average earthward velocity from the THB observations, and a ~8 min propagation time starting from ~0523 UT, the initiation time of the second auroral intensification and of the flow at THB, to the auroral fading at ~0531 UT, the flow may have propagated to X ~−11 R_E. This is consistent with this N-S arc not reaching the equatorward edge of the aurora oval. The substorm onset connected to the fourth intensification had a small auroral expansion, which occurred well

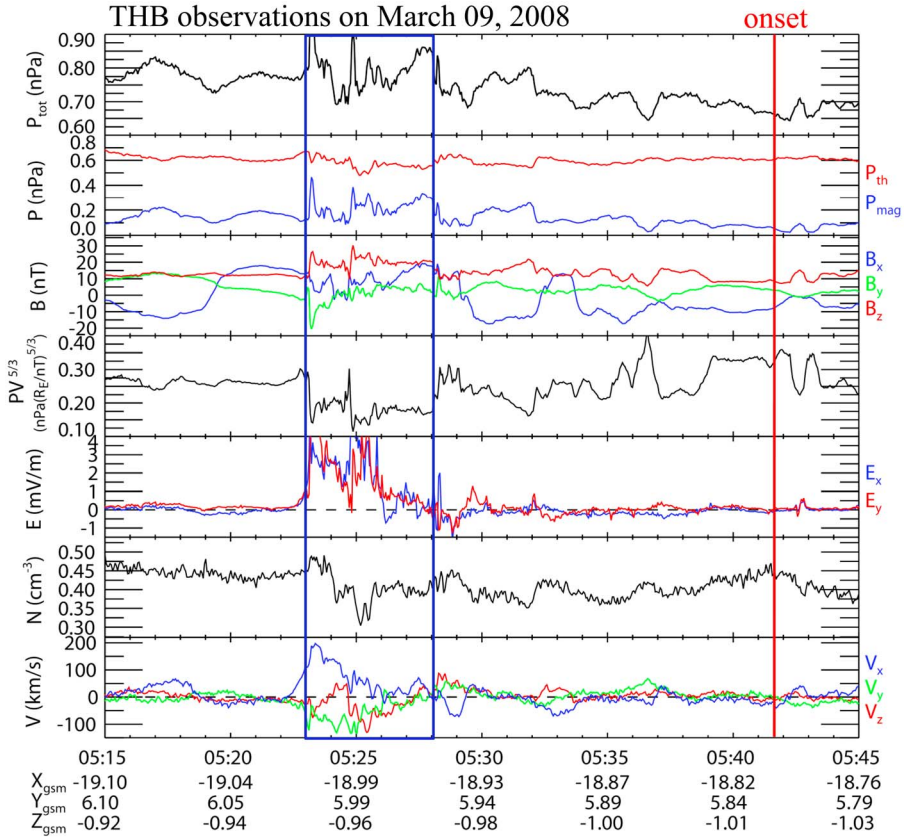

Figure 4. The THB spacecraft observations in the plasma sheet on 9 March 2008 between 0515 and 0545 UT, corresponding to the aurora observations shown in Figure 3. The panels show total pressure, plasma and magnetic pressures, magnetic field, entropy parameter ($PV^{5/3}$), electric field, ion density, and plasma bulk flow velocity in the GSM coordinates.

equatorward and eastward of the THB footprint region. Thus, no onset signature was observed by THB. The more earthward spacecraft THC observed flow channel signatures corresponding to other aurora arcs, which did not lead to the substorm onset. Those flow channels are not considered here.

[19] These two events showed that the preonset fast flow channels associated with reduced pressure and flux tube volume, which suggests low-entropy plasma, can be observed in the midtail plasma sheet. The next two events show the signatures for the fast flow channels in the near-Earth plasma sheet at R ~11 R_E, which is very close to the onset initiation region. Figure 5 shows six selected images of the THEMIS ASI images during a substorm event preceded by a PBI and N-S aurora arc ~4 min before onset on 29 February 2008, which is the first event shown by *Nishimura et al.* [2010]. In this case, the PBI initiated near the center of the FSMI FOV near 68° MLAT. The N-S auroral arc followed the PBI and reached the growth phase arc in the ATHA FOV, leading to a substorm onset at ~0822 UT equatorward of ~65° MLAT. The T96 magnetic field model mapping of the spacecraft THD footprint range is marked by the cyan rectangle in the third image, which shows the N-S arc proceeding equatorward. Any evidence of a flow channel would be expected to be observed by THD and possibly THE several minutes before an onset signature.

[20] Figure 6 shows the THD observations of the total pressure, plasma and magnetic pressures, magnetic field, electric field, and **E** × **B** drift velocity, respectively, from 0800 to 0840 UT on 29 February 2008. The vertical red line identifies the substorm onset time at ~0821:30 UT determined by the ASIs observation. The blue rectangle represents the time interval between the initiation of the N-S aurora arc equatorward motion and the onset brightening. The three pressure curves show a plasma sheet stretching lasting more than 10 min before the substorm onset. The total pressure shows a notable reduction resulting from a magnetic field change starting ~3 min before the onset, when the N-S arc was observed to move across the spacecraft footprint range. This correspondence suggests that a fast flow channel with lower plasma content moved underneath the spacecraft in the plasma sheet. A substantial duskward electric field enhancement is found to be associated with the pressure reduction, which represents the electric field variation when the fast flow channel extended to the magnetic field line of the spacecraft location. An **E** × **B** drift flow from the lobe toward the central plasma sheet enhanced to several tens of kilometers per second before the onset occurred, which indicates the continuous earthward transport of plasma from the more distant tail penetrating into the near-Earth region prior to the onset.

[21] Figure 7 shows the same quantities obtained from the probe THE, which is located ~1 R_E west of THD. The flow channel in the plasma sheet is captured by the total pressure reduction, which is identical to THD. However, the electric

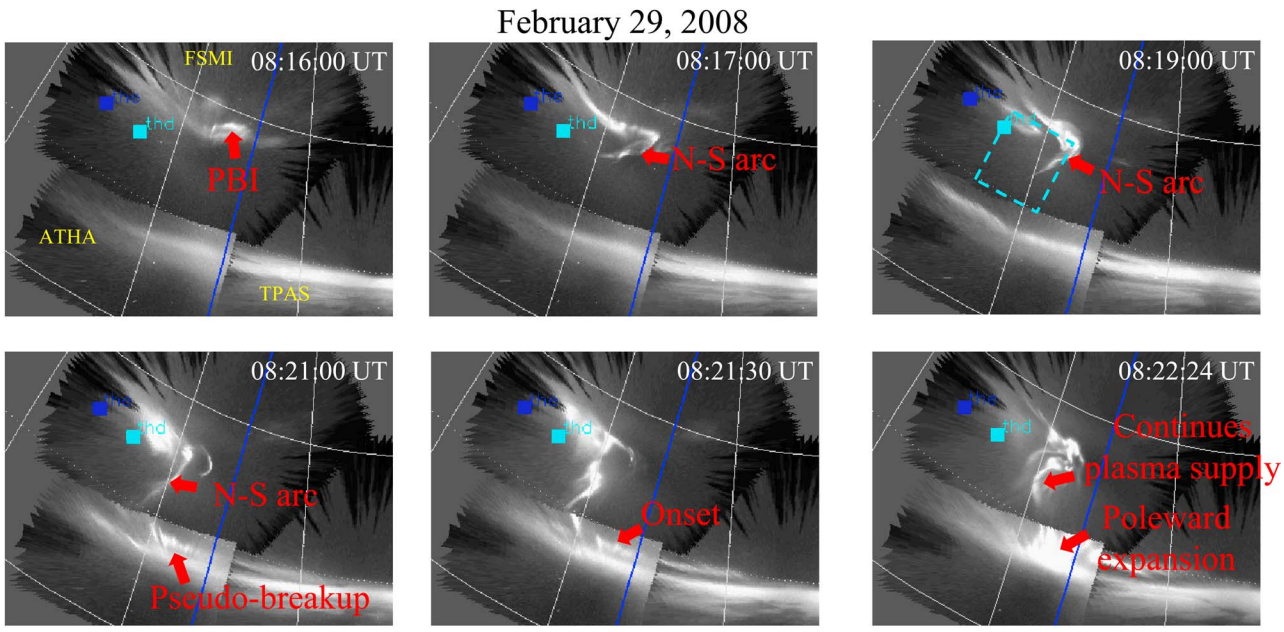

Figure 5. Snapshots of THEMIS ASI observations on 29 February 2008. The substorm onset occurred at 0821:30 UT.

field and the perpendicular flow show only very small changes. This may indicate that the continuous supplying of depleted plasma flows were confined to the flux tubes mapping to the east of THE, and that THE was on the edge of the azimuthally localized flow channel. The preonset pressure reduction is followed by the onset pressure reduction immediately, which suggests that the footprints of the two spacecraft should be mapped to near the equatorward edge of the rectangle in Figure 5, just poleward of the initial aurora onset expansion region. The timing of the flow channel propagation cannot be estimated for this case due to the measurement being well away from the central plasma sheet.

[22] Similar flow channel signatures are captured in the inner plasma sheet during another event that occurred in the

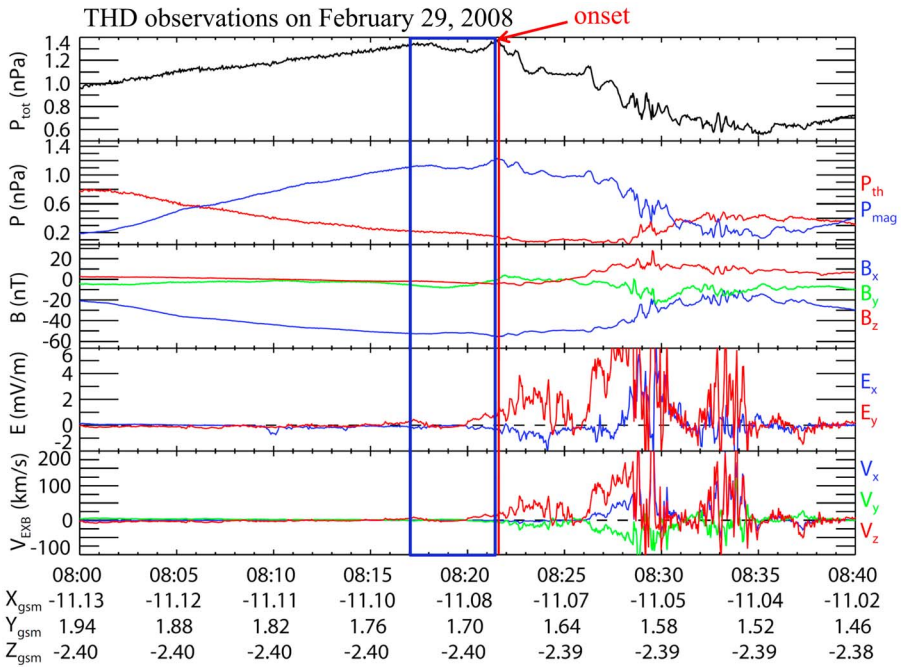

Figure 6. The THD spacecraft observations in the lobe on 29 February 2008 between 0800 and 0840 UT, corresponding to the aurora observations shown in Figure 5. The panels show total pressure, thermal and magnetic pressures, magnetic field, electric field, and **E** × **B** drift velocity in GSM coordinate.

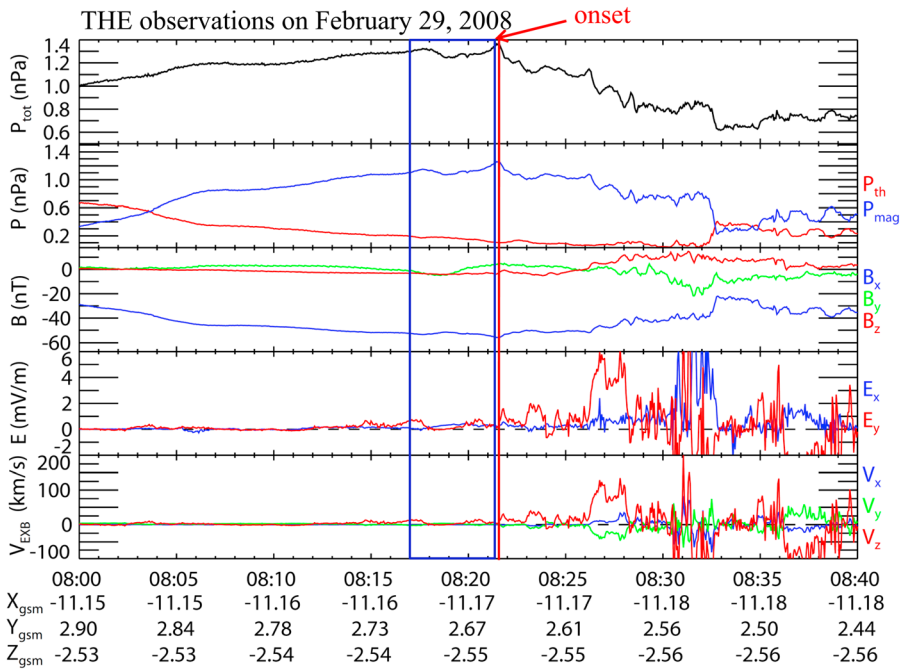

Figure 7. The THE spacecraft observations in the lobe on 29 February 2008 between 0800 and 0840 UT. The format is the same as Figure 6.

premidnight region. Figure 8 shows six selected ASI images for a preonset N-S auroral arc event on 16 March 2008. The IMF was quite stable during this period, so only the instantaneous spacecraft locations are shown. The faint arc is first observed ~4 min before the substorm onset in the FSMI FOV. It moved across the footprints of THD and THE spacecraft less than 1 min before the onset brightening. Note that the arc intensification seen between ~0627 and ~0629 UT in the western part of FSIM image FOV may have been a pseudo-breakup. It did not expand poleward or azimuthally toward the spacecraft and quickly disappeared.

[23] Figure 9 shows the THD observation given in the same format as Figures 6 and 7. The spacecraft was located near the lobe before the onset. The total pressure in the first panel shows a small but noticeable reduction ~30 s before the substorm onset, as seen in the event shown in Figures 6

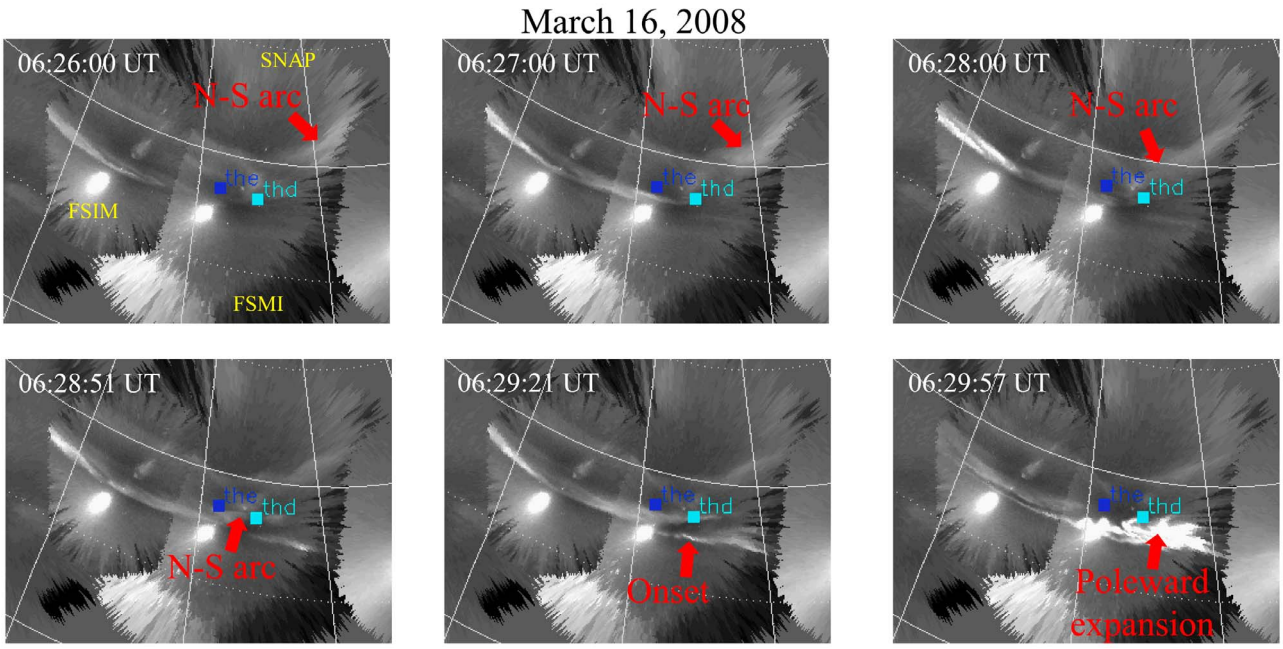

Figure 8. Snapshots of THEMIS ASI observations on 16 March 2008. The substorm onset occurred at 0629:21 UT.

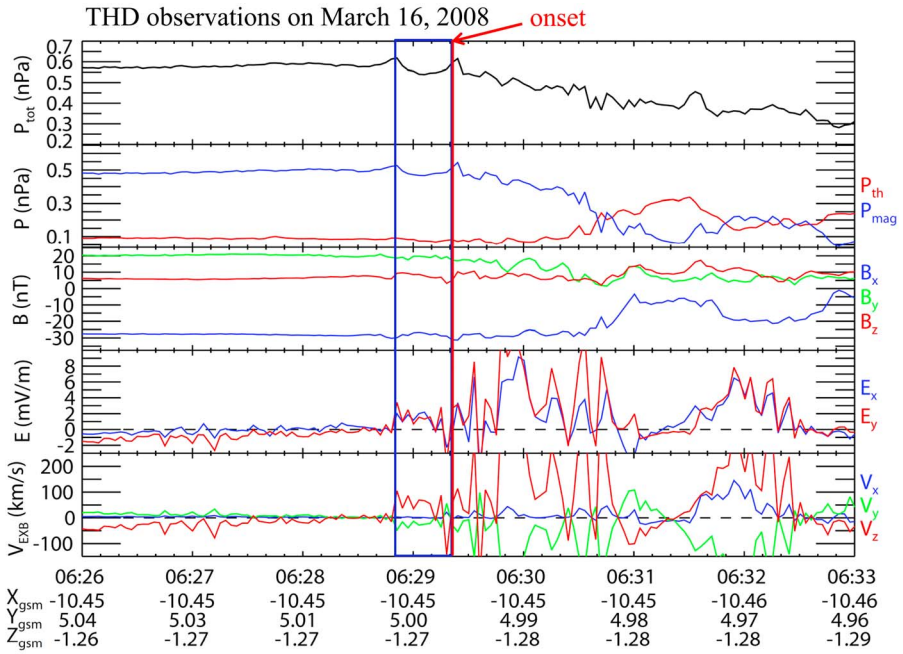

Figure 9. The THD spacecraft observations in the lobe on 16 March 2008 between 0626 and 0633 UT, corresponding to the aurora observations shown in Figure 8. The format is the same as Figures 6 and 7.

and 7. The magnetic field in the third panel show a transient change toward a more dipolarized configuration, which may suggest the local expansion of the plasma sheet affected by the flux tubes associated with the underpopulated plasma. The electric field shows almost simultaneous enhancement in both the x and y directions, which is related to an enhancement of $\mathbf{E} \times \mathbf{B}$ ion flows toward the central plasma sheet. Since the spacecraft was located very close to the outer boundary of the plasma sheet due to the plasma sheet thinning, this flow is expected to be associated with an earthward flow enhancement near the equator further down the tail.

[24] THE probe located ~1 R_E west of THD observed slightly different signatures. Figure 10 shows that both the preonset and substorm pressure changes at THE were captured ~15 s later than those at THD, which is consistent with the equatorward and westward motion of the preonset arc

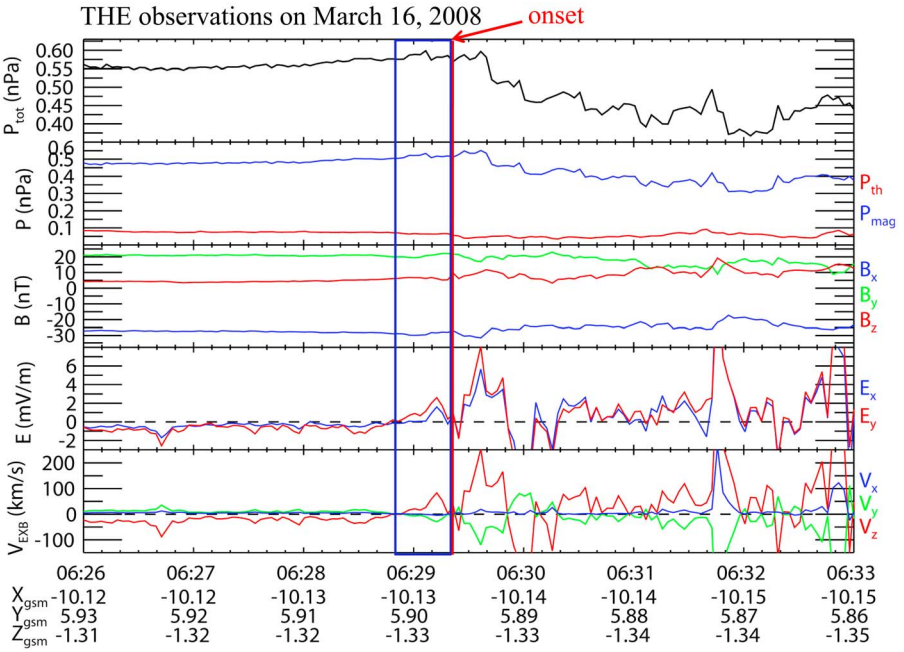

Figure 10. The THE spacecraft observations in the lobe on 16 March 2008 between 0626 and 0633 UT. The format is the same as Figures 6, 7, and 9.

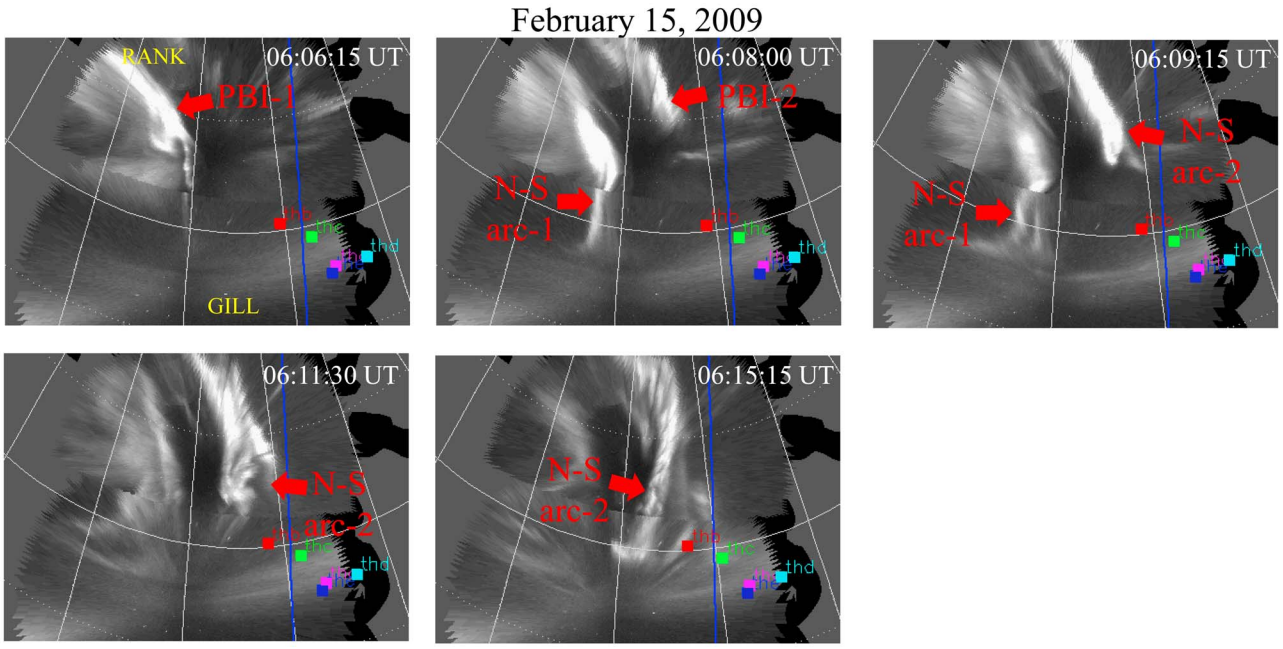

Figure 11. Snapshots of THEMIS ASI observations on 15 February 2009. Two aurora north-south arcs are observed with four spacecraft footprints mapped to their vicinity. No substorm occurred during this time period.

and the westward expansion of the onset brightening observed from the aurora image. The pressure reduction ~30 s prior to the onset is consistent with that observed by THD, except that the preonset reduction at THE is quite small. This small pressure reduction at THE suggests that the penetrated flow channel was localized and located mostly to the east of THE. The electric field and the **E** × **B** drift in the fourth and fifth panel show simultaneous enhancements as the N-S aurora arc moved across the spacecraft footprint, representing the continuous flow intruding. As for the previous event, the preonset timing cannot be estimated because the measurement was far away from the central plasma sheet.

[25] Present THEMIS spacecraft observations provide a limited number of conjunction events due to the small spatial scale in azimuth of the transient preonset flow channel. However, the good conjunction events (as detailed previously) show clear evidence for a one-to-one correlation between the earthward penetrations of the fast flow channels associated with reduced entropy plasma into the near-Earth plasma sheet region prior to the substorm onset and the N-S aurora arcs traveling equatorward toward the growth phase arc preceding to the onset brightening. These preonset flow channel characteristics resemble the earthward transport of reduced-entropy plasma bubbles after substorm onset [e.g., *Sergeev et al.*, 1996; *Runov et al.*, 2009; *Yang et al.*, 2010]. However, the signatures for preonset flow channels are weaker and probably smaller in spatial scale. These preonset low-entropy flow channels could result from the enhanced reduced-entropy plasma transport across the plasma sheet boundary toward the central plasma sheet, consistent with what we see for the third and the fourth events shown in Figures 5 and 8 above. Ionospheric counterpart observations have found that the preonset equatorward flow enhancements cross the polar cap boundary [*Lyons et al.*, 2010], which may supply low-entropy plasma to the plasma sheet before onset. These cross-separatrix flows could be associated with enhanced local reconnection tailward of the spacecraft location. However, direct observations are needed to support this connection. The timing issue of the flow channel is also consistent with the ground radar observations [*Lyons et al.*, 2010]. These observation results lead to a conclusion that the preonset flow channel may play an important role in the substorm triggering process.

3.2. N-S Auroral Arc Not Associated With Substorm Onset

[26] N-S auroral structures are found not only prior to substorm onsets, but also frequently during other times. We do not expect there to be a substantial difference between the flow channel for these cases and the preonset arcs. Figure 11 shows selected THEMIS ASI images from RANK and GILL on 15 February 2009. Only the instantaneous spacecraft footprints are shown because the IMF was steady during this period. There are two N-S auroral arcs separated by ~1 MLT, with one following the other, identified between ~0604 and ~0620 UT. The first aurora intensification initiated at ~0604:15 UT in the RANK FOV with the equatorward portion extending into the GILL FOV. As this first arc moved toward the equator, the second arc intensified in the poleward portion of the RANK FOV at ~0607 UT to the east of the first arc. The narrow front of the first arc approached a preexisting east-west arc slightly poleward of the auroral oval equatorward boundary in the midportion of the GILL FOV, and then turned westward while the trailing part of the arc continuously moved equatorward. It gradually dissipated while moving westward, during which time the second arc proceeded equatorward. The second arc weakened in intensity as it moved equatorward. The footprints of the five spacecraft

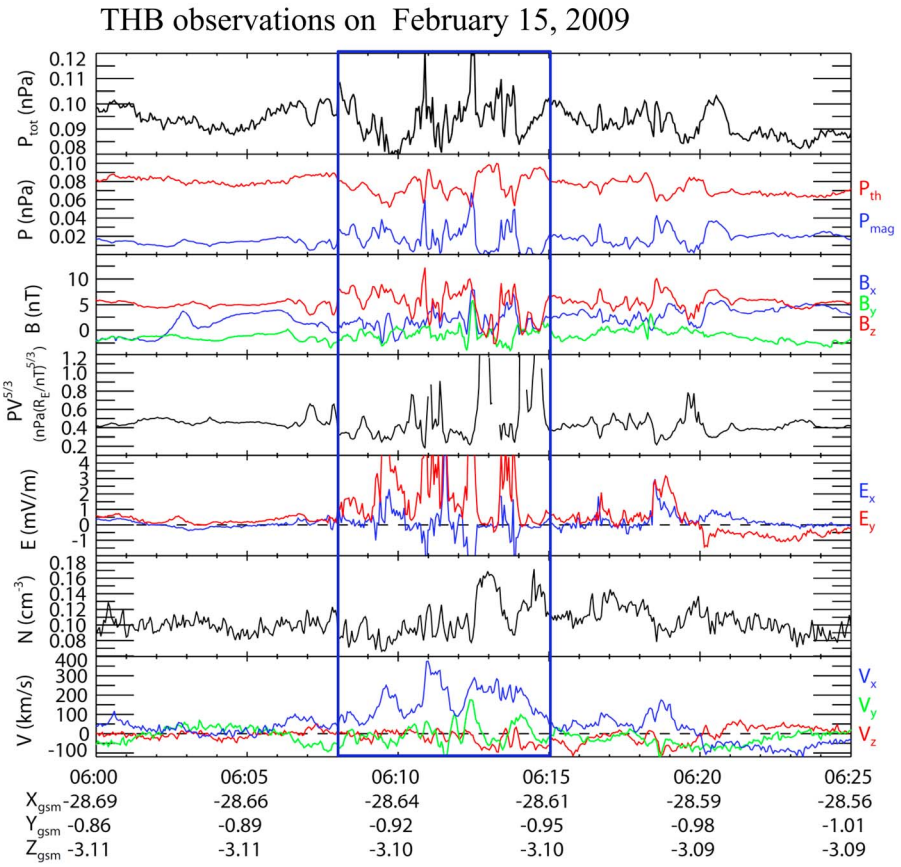

Figure 12. The THB spacecraft observations in the plasma sheet on 15 February 2009 between 0600 and 0625 UT, corresponding to the aurora observations shown in Figure 11. The format is the same as Figure 4.

were mapped >1 MLT east of the first N-S arc and within 1 MLT east of the second arc with THB being the closest.

[27] Figure 12 shows the observations of total pressure, thermal and magnetic pressures, magnetic field, entropy parameter, electric field, ion number density, and ion bulk flow velocity observed by THB, which was located at X ~−29 R_E near midnight. The blue rectangle marks the time interval that the substantial changes were observed by THB. Associated with the first aurora arc moving equatorward about 1 MLT west of the spacecraft footprint, a total pressure reduction was observed starting from ~0608 UT. This would place the flow channel ~5 to 6 R_E in Y_{GSM} dawnward of the mapping of the arc to the plasma sheet, which is consistent with the <10 R_E azimuthal width of bursty flows in the plasma sheet suggested by *Angelopoulos et al.* [1992]. The second arc moved close to the THB footprint and brought two other pressure drops at ~0611:00 and ~0612:30 UT with many fluctuations. All of these reductions were associated with substantial reduction of the plasma thermal pressure. Associated with the pressure reductions, the magnetic field B_z component increased slightly, though with strong fluctuations. $PV^{5/3}$ in the fourth panel exhibits a reduction with fluctuations during the time periods that the two aurora arcs passed by the spacecraft footprint. The $PV^{5/3}$ fluctuations correspond to the magnetic field B_z fluctuations and are related to the magnetic field topology change. Substantial duskward electric field enhancements are associated with the pressure and $PV^{5/3}$ reductions. The ion number density was slightly reduced during this time interval. The ion bulk flow velocity shows a strong earthward enhancement during the time of the pressure and entropy reduction and the duskward electric field increase.

[28] There are some flow enhancements observed 2–3 min before the major signatures, which may represent the flow perturbation from the narrow front of the first flow channel without THB moving into that flow channel. The narrow front of the first arc reached the THB footprint latitude at ~0606:30 UT, which is consistent with the initial flow enhancement observed by THB starting from ~0605:10 UT, allowing ~80 s Alfven transit time. This arc front reached ~68° MLAT and turned westward at ~0607:15 UT. Using the ~100 km/s average earthward transport velocity from the THB observations, the flow channel could penetrate only as earthward as X ~−27 R_E, indicating that it is likely that THB did not fully enter this flow channel. The second arc reached THB footprint latitude at ~0611:30 UT, corresponding to the flow enhancement starting from ~0610:10 UT at THB. This arc reached lower magnetic latitude at ~0619:00 UT. Assuming ~200 km/s average propagating time according to THB observation, this arc may have reached X ~−14 R_E.

[29] THC, located earthward and eastward of THB, observed much weaker but similar signatures at X ~−18 R_E between ~0616 and ~0618 UT (not shown), which suggests

a deceleration and gradual dissipation of the flow channel. The other three spacecraft located at X ~−10 R_E and further east did not observe any substantial changes, which likely reflects the localized structure of the flow channel. These multispacecraft observations suggest that localized low-entropy flux tubes penetrate earthward at moderate speeds during nonsubstorm periods and could affect the radial gradient of entropy within the plasma sheet and play an important role in resolving the pressure balance inconsistency [e.g., *Erickson and Wolf*, 1980; *Garner et al.*, 2003; *Xing and Wolf*, 2007; *Wolf et al.*, 2009]. This event also suggests that the reduced-entropy flow channels are not sufficient triggers for substorm onset. Possible necessary conditions are discussed in section 4.

4. Summary

[30] We have taken advantage of the THEMIS spacecraft conjunction with the N-S auroral arcs and found a distinct correlation between the azimuthally localized N-S auroral arcs and moderate speed earthward flow channels in the plasma sheet. Four preonset flow channel events are presented, two observed in the midtail plasma sheet and the other two observed in the near-Earth plasma sheet. The flow channel characteristics are consistent with the plasma bubbles that were proposed by *Chen and Wolf* [1993]. Substantial entropy parameter and pressure reduction in the flow channel have been found to be associated with small-scale dipolarizations, substantial duskward electric field enhancements, and earthward flow enhancements. This correlation combined with the high occurrence of preonset auroral structure observed by *Nishimura et al.* [2010] suggests that the preonset reduced-entropy fast flow channels may play a crucial role in disturbing the inner plasma sheet region, where the substorm onset is suggested to be initiated [*Jacquey et al.*, 1991, 1993; *Samson et al.*, 1992; *Ohtani et al.*, 1992], leading to the substorm onset. The timing for the flow channel to transport plasma to the plasma sheet inner boundary has been found to be consistent with the preonset aurora observations.

[31] We also found that similar flow channels correlated with N-S auroral arcs can appear during quiet times and not lead to the substorm onset. This suggests that the earthward penetration of reduced-entropy fast flow channels is not a sufficient condition for an onset to occur. We suggest two necessary preconditions for the onset. First is the buildup of plasma pressure and azimuthal pressure gradient associated with the formation of the Harang reversal in the inner plasma sheet near the premidnight region. It has been suggested that during the growth phase the inner plasma sheet pressure is enhanced dramatically due to enhanced convection and builds up a pressure peak in the premidnight sector, resulting from the ion gradient curvature drift [e.g., *Lemon et al.*, 2004; *Gkioulidou et al.*, 2009]. The high-pressure gradient region associated with the overlap of the opposite polarity of the region 2 field-aligned current forms the Harang reversal [*Gkioulidou et al.*, 2009], which is suggested to be near the location where substorm onset is initiated [*Bristow et al.*, 2001, 2003; *Zou et al.*, 2009]. Thus, we suggest it is possible that even though the reduced-entropy fast flow channel reaches the preexisting arc, substorm onset may not be ignited due to insufficient pressure and azimuthal pressure gradient.

[32] The second possible necessary condition is that the entropy reduction in the fast flow channel is sufficiently low for the channel to penetrate earthward to reach the critical region in the inner plasma sheet where the preonset pressure enhancement and azimuthal pressure gradient has been set up, which introduces perturbations into this region and causes instability of the plasma sheet. For example, it is shown in event 2 (Figures 3 and 4) that the substorm onset was initiated after the fourth auroral intensification approached the preexisting arc instead of any of the first three intensifications along the same channel. The aurora images show that the first three intensifications associated with the flow channel did not contact with the preexisting arc. We speculate that the entropy of these flow channel fronts was not depleted sufficiently, and thus the channels achieved the interchange stability against neighboring flux tubes before reaching the inner plasma sheet boundary. Under this idea, the continuous new plasma supply along the same flow channel, identified as the fourth intensification, provided low enough entropy plasma and reached the inner plasma sheet to lead to the substorm onset.

[33] The physical mechanism of the substorm onset being triggered near the plasma sheet inner boundary and the role of the reduced-entropy fast flow channel are still open questions. Nevertheless, the observational evidence presented here strongly suggests that the new plasma intrusion into the inner plasma sheet boundary may bring crucial entropy changes and lead to onset instability. Further studies are needed for more details of the substorm time sequence. For example, distant magnetotail observations are essential to explore the location and mechanism of the flow channel initiation, numerical simulations will help to quantify the entropy reduction required for the sufficient flow channel penetration, and instability analyses are needed to reveal the physics of the perturbation relation between the penetrated reduced-entropy flow channel and the plasma in the inner plasma sheet region.

[34] **Acknowledgments.** This work at UCLA was supported by National Science Foundation grants ATM-0639312 and ATM-0646233 and NASA grant NNX09AI06G. THEMIS is funded by NASA contract NAS5-02099. Deployment of the THEMIS ASIs was partly supported by CSA contract 9F007-046101. OMNI solar wind data were provided through the Coordinated Data Analysis Web. We greatly thank J. McFadden for providing THEMIS ESA data.

[35] Robert Lysak thanks Joachim Birn and another reviewer for their assistance in evaluating this paper.

References

Angelopoulos, V. (2008), The THEMIS mission, *Space Sci. Rev.*, Vol. 141, Numbers 1–4, 5–34, doi:10.1007/s11214-008-9336-1.

Angelopoulos, V., W. Baumjohann, C. F. Kennel, F. V. Coroniti, M. G. Kivelson, R. Pellat, R. J. Walker, H. Lühr, and G. Paschmann (1992), Bursty bulk flows in the inner central plasma sheet, *J. Geophys. Res.*, *97*(A4), 4027–4039, doi:10.1029/91JA02701.

Angelopoulos, V., C. F. Kennel, F. V. Coroniti, R. Pellat, M. G. Kivelson, R. J. Walker, C. T. Russell, W. Baumjohann, W. C. Feldman, and J. T. Gosling (1994), Statistical characteristics of bursty bulk flow events, *J. Geophys. Res.*, *99*(A11), 21,257–21,280, doi:10.1029/94JA01263.

Angelopoulos, V., et al. (2008), Tail reconnection triggering substorm onset, *Science*, *321*, 931–935, doi:10.1126/science.1160495.

Auster, H. U., et al. (2008), The THEMIS fluxgate magnetometer, *Space Sci. Rev.*, *141*, 235–264, doi:10.1007/s11214-008-9365-9.

Baumjohann, W., G. Paschmann, and H. Lühr (1990), Characteristics of high-speed ion flows in the plasma sheet, *J. Geophys. Res.*, *95*(A4), 3801–3809, doi:10.1029/JA095iA04p03801.

Bonnell, J. W., F. S. Mozer, G. T. Delory, A. J. Hull, R. E. Ergun, C. M. Cully, V. Angelopoulos, and P. R. Harvey (2008), The electric field instrument (EFI) for THEMIS, *Space Sci. Rev.*, *141*, 303–341, doi:10.1007/s11214-008-9469-2.

Bristow, W. A., A. Otto, and D. Lummerzheim (2001), Substorm convection patterns observed by the Super Dual Auroral Radar Network, *J. Geophys. Res.*, *106*(A11), 24,593–24,609, doi:10.1029/2001JA000117.

Bristow, W. A., G. J. Sofko, H. C. Stenbaek-Nielsen, S. Wei, D. Lummerzheim, and A. Otto (2003), Detailed analysis of substorm observations using SuperDARN, UVI, ground-based magnetometers, and all-sky imagers, *J. Geophys. Res.*, *108*(A3), 1124, doi:10.1029/2002JA009242.

Chen, C. X., and R. A. Wolf (1993), Interpretation of high-speed flows in the plasma sheet, *J. Geophys. Res.*, *98*(A12), 21,409–21,419, doi:10.1029/93JA02080.

Erickson, G. M., and R. A. Wolf (1980), Is steady convection possible in the Earth's magnetotail?, *Geophys. Res. Lett.*, *7*(11), 897–900, doi:10.1029/GL007i011p00897.

Escoubet, C. P., R. Schmidt, and M. L. Goldstein (1997), Cluster—Science and mission overview, *Space Sci. Rev.*, *79*(1–2), 11–32, doi:10.1023/A:1004923124586.

Fairfield, D., et al. (1999), Earthward flow bursts in the inner magnetotail and their relation to auroral brightenings, AKR intensifications, geosynchronous particle injections and magnetic activity, *J. Geophys. Res.*, *104*(A1), 355–370, doi:10.1029/98JA02661.

Garner, T. W., R. A. Wolf, R. W. Spiro, M. F. Thomsen, and H. Korth (2003), Pressure balance inconsistency exhibited in a statistical model of magnetospheric plasma, *J. Geophys. Res.*, *108*(A8), 1331, doi:10.1029/2003JA009877.

Gkioulidou, M., C.-P. Wang, L. R. Lyons, and R. A. Wolf (2009), Formation of the Harang reversal and its dependence on plasma sheet conditions: Rice convection model simulations, *J. Geophys. Res.*, *114*, A07204, doi:10.1029/2008JA013955.

Henderson, M. G., G. D. Reeves, and J. S. Murphree (1998), Are north-south aligned auroral structures an ionospheric manifestation of bursty bulk flows?, *Geophys. Res. Lett.*, *25*(19), 3737–3740, doi:10.1029/98GL02692.

Jacquey, C., J. A. Sauvaud, and J. Dandouras (1991), Location and propagation of the magnetotail current disruption during a substorm expansion: Analysis and simulation of an ISEE multi-onset event, *Geophys. Res. Lett.*, *18*(3), 389–392, doi:10.1029/90GL02789.

Jacquey, C., J. A. Sauvaud, J. Dandouras, and A. Korth (1993), Tailward propagating cross-tail current disruption and dynamics of near-Earth tail: A multi-point measurement analysis, *Geophys. Res. Lett.*, 428 *20*(10), 983–986, doi:10.1029/93GL00072.

Kauristie, K., V. A. Sergeev, O. Amm, M. V. Kubyshkina, J. Jussila, E. Donovan, and K. Liou (2003), Bursty bulk flow intrusion to the inner plasma sheet as inferred from auroral observations, *J. Geophys. Res.*, *108*(A1), 1040, doi:10.1029/2002JA009371.

Lemon, C., R. A. Wolf, T. W. Hill, S. Sazykin, R. W. Spiro, F. R. Toffoletto, J. Birn, and M. Hesse (2004), Magnetic storm ring current injection modeled with the Rice Convection Model and a self-consistent magnetic field, *Geophys. Res. Lett.*, *31*, L21801, doi:10.1029/2004GL020914.

Lui, A. T. Y. (2008), Comment on "Tail Reconnection Triggering Substorm Onset", *Science*, *324*, 1391, doi:10.1126/science.1167726.

Lyons, L. R. (1995), A new theory for magnetospheric substorms, *J. Geophys. Res.*, *100*(A10), 19,069–19,081, doi:10.1029/95JA01344.

Lyons, L. R., T. Nagai, G. T. Blanchard, J. C. Samson, T. Yamamoto, T. Mukai, A. Nishida, and S. Kokobun (1999), Association between Geotail plasma flows and auroral poleward boundary intensifications observed by CANOPUS photometers, *J. Geophys. Res.*, *104*(A3), 4485–4500, doi:10.1029/1998JA900140.

Lyons, L. R., Y. Nishimura, Y. Shi, S. Zou, H.-J. Kim, V. Angelopoulos, C. Heinselman, M. J. Nicolls, and K.-H. Fornacon (2010), Substorm triggering by new plasma intrusion: Incoherent-scatter radar observations, *J. Geophys. Res.*, *115*, A07223, doi:10.1029/2009JA015168.

McFadden, J. P., C. W. Carlson, D. Larson, M. Ludlam, R. Abiad, B. Elliott, P. Turin, M. Marckwordt, and V. Angelopoulos (2008), The THEMIS ESA plasma instrument and in-flight calibration, *Space Sci. Rev.*, *141*, 277–302, doi:10.1107/s11214-008-9440-2.

McPherron, R. L., C. T. Russell, and M. Aubry (1973), Satellite studies of magnetospheric substorms on August 15, 1968, 9. Phenomenological model for substorms, *J. Geophys. Res.*, *78*(16), 3131–3149, doi:10.1029/JA078i016p03131.

Nakamura, R., W. Baumjohann, R. Schödel, M. Brittnacher, V. Sergeev, M. Kubyshkina, T. Mukai, and K. Liou (2001), Earthward flow bursts, auroral streamers, and small expansions, *J. Geophys. Res.*, *106*(A6), 10,791–10,802, doi:10.1029/2000JA000306.

Nishimura, Y., L. Lyons, S. Zou, V. Angelopoulos, and S. Mende (2010), Substorm triggering by new plasma intrusion: THEMIS all-sky imager observations, *J. Geophys. Res.*, *115*, A07222, doi:10.1029/2009JA015166.

Ohtani, S., S. Kokubun, and C. T. Russell (1992), Radial expansion of the tail current disruption during substorms: A new approach to the substorm onset region, *J. Geophys. Res.*, *97*(A3), 3129–3136, doi:10.1029/91JA02470.

Pontius, D. H., Jr., and R. A. Wolf (1990), Transient flux tubes in the terrestrial magnetosphere, *Geophys. Res. Lett.*, *17*(1), 49–52, doi:10.1029/GL017i001p00049.

Runov, A., V. Angelopoulos, M. I. Sitnov, V. A. Sergeev, J. Bonnell, J. P. McFadden, D. Larson, K.-H. Glassmeier, and U. Auster (2009), THEMIS observations of an earthward-propagating dipolarization front, *Geophys. Res. Lett.*, *36*, L14106, doi:10.1029/2009GL038980.

Samson, J. C., L. R. Lyons, B. Xu, F. Creutzberg, and P. Newell (1992), Proton aurora and substorm intensifications, *Geophys. Res. Lett.*, *19*(21), 2167–2170, doi:10.1029/92GL02184.

Schmidt, G. (1979), *Physics of High Temperature Plasmas*, 2nd ed., 420 pp., Academic, New York.

Sergeev, V. A., V. Angelopoulos, J. T. Gosling, C. A. Cattell, and C. T. Russell (1996), Detection of localized, plasma-depleted flux tubes or bubbles in the midtail plasma sheet, *J. Geophys. Res.*, *101*(A5), 10,817–10,826, doi:10.1029/96JA00460.

Sergeev, V. A., K. Liou, C.-I. Meng, P. T. Newell, M. Brittnacher, G. Parks, and G. D. Reeves (1999), Development of auroral streamers in association with localized impulsive injections to the inner magnetotail, *Geophys. Res. Lett.*, *26*(3), 417–420, doi:10.1029/1998GL900311.

Tsyganenko, N. A., and D. P. Stern (1996), Modeling the global magnetic field of the large-scale Birkeland current systems, *J. Geophys. Res.*, *101*(A12), 27,187–27,198, doi:10.1029/96JA02735.

Volkov, M. A., and Y. P. Mal'tsev (1986), A slot instability of the inner boundary of the plasma layer, *Geomag. Aeron.*, *26*(5), 671–673.

Wolf, R. A., V. Kumar, F. R. Toffoletto, G. M. Erickson, A. M. Savoie, C. X. Chen, and C. L. Lemon (2006), Estimating local plasma sheet $PV^{5/3}$ from single-spacecraft measurements, *J. Geophys. Res.*, *111*, A12218, doi:10.1029/2006JA012010.

Wolf, R. A., Y. Wan, X. Xing, J.-C. Zhang, and S. Sazykin (2009), Entropy and plasma sheet transport, *J. Geophys. Res.*, *114*, A00D05, doi:10.1029/2009JA014044.

Xing, X., and R. A. Wolf (2007), Criterion for interchange instability in a plasma connected to a conducting ionosphere, *J. Geophys. Res.*, *112*, A12209, doi:10.1029/2007JA012535.

Yang, J., F. R. Toffoletto, G. M. Erickson, and R. A. Wolf (2010), Superposed epoch study of PV5/3 during substorms, pseudobreakups and convection bays, *Geophys. Res. Lett.*, *37*, L07102, doi:10.1029/2010GL042811.

Zesta, E., E. Donovan, L. Lyons, G. Enno, J. S. Murphree, and L. Cogger (2002), Two-dimensional structure of auroral poleward boundary intensifications, *J. Geophys. Res.*, *107*(A11), 1350, doi:10.1029/2001JA000260.

Zou, S., L. R. Lyons, C.-P. Wang, A. Boudouridis, J. M. Ruohoniemi, P. C. Anderson, P. L. Dyson, and J. C. Devlin (2009), On the coupling between the Harang reversal evolution and substorm dynamics: A synthesis of SuperDARN, DMSP, and IMAGE observations, *J. Geophys. Res.*, *114*, A01205, doi:10.1029/2008JA013449.

V. Angelopoulos, Institute of Geophysics and Planetary Physics/Earth and Space Sciences, University of California, Los Angeles, Los Angeles, CA 90095-1567, USA.

U. Auster, Institut für Geophysik und Extraterrestrische Physik der TUBM Mendelsohnstrasse 3, Braunschweig, D-38106, Germany.

J. Bonnell, C. Carlson, and D. Larson, Space Sciences Laboratory, University of California, Berkeley, Berkeley, CA 94720-7450, USA.

L. Lyons, X. Xing, and Y. Nishimura, Department of Atmospheric and Oceanic Science, University of California, Los Angeles, Los Angeles, CA 90095-1567, USA. (xyxingchen@gmail.com)